Journal of Photochemistry, 9 (1978) 369 - 383

RECOMBINATION OF LEAD ATOMS

P. J. CROSS and D. HUSAIN

The Department of Physical Chemistry, The University of Cambridge, Lensfield Road, Cambridge CB2 1EP (Gt. Britain)

(Received February 14, 1978)

Summary

The recombination of ground state lead atoms $Pb(6^3P_0)$ is considered from the experimental and theoretical viewpoints. Experiments were carried out in which the atom was monitored by resonance line absorption at λ = 283.3 nm ($Pb(7s(^3P_1^0) \leftarrow 6p^2(^3P_0))$) following the pulsed irradiation of lead tetraethyl in the presence of CO_2. A computational analysis of the photoelectric pulses was carried out assuming the presence of kinetic components in both [Pb] and $[Pb]^2$. It was found that the high sensitivity of this method prevents extraction of the component of the rate involving $[Pb]^2$ from the measured decays. This is seen to be a general limitation on the study of the recombination of atoms derived from the pulsed photolysis of a large molecule. Rate constants for the process Pb + Pb + M → Pb_2 + M have been calculated using the variational phase space theory of Keck for M = He, Ne, Ar, Kr, Xe, O_2, N_2, CO_2, CH_4, C_2H_6, CF_4 and SF_6. The resulting data are discussed within the context of previous studies on the rates of nucleation of lead vapours.

1. Introduction

The study of the recombination rates of two atoms to form a diatomic molecule is an area highly developed from both the experimental [1] and theoretical viewpoints [2, 3]. From the experimental viewpoint, the main emphasis has clearly been on the study of the recombination of atoms to form stable diatomic molecules such as the molecular halogens, H_2, O_2 and N_2. One reason for this is the clear convenience afforded by the ease of establishing a material balance and the determination of absolute atomic concentrations from monitoring a molecular property that can be readily calibrated, such as a molecular optical extinction coefficient. By obvious contrast few, if any, detailed investigations of the kinetics of metal atom recombination have been undertaken. Such processes are of interest *per se* and are also of practical concern since the rates of the initial recombination of two atoms may govern the overall formation rates of smokes from metal

atom vapours. An example of this is the production of particulate lead from the shock-tube-initiated thermal decomposition of lead tetramethyl [4].

We have described previously [5 - 8] a number of kinetic studies in which the ground state lead atom $Pb(6^3P_0)$ has been monitored directly in the time resolved mode. In these studies $Pb(6^3P_0)$ was generated photochemically from low pressures of lead tetraethyl ($PbEt_4$) and monitored by atomic resonance line absorption. The collisional behaviour of ground state lead atoms is of fundamental interest since it constitutes part of an overall programme of the kinetic study of group IV atoms (C to Pb) where the role of increasing spin–orbit coupling is investigated [9]. The recombination process is of special relevance to the chemical mechanism of the effect of added $PbEt_4$ (anti-knock) to the internal combustion engine. In this paper we describe (a) an attempted experimental investigation to determine atomic recombination rates from resonance line absorption and (b) calculations of lead atom recombination rates using the phase space theory of Keck [10, 11]. The extraction of the kinetic component, which is second order in atomic concentration, in experiments in which transient atoms are generated from the pulsed photolysis of relatively large molecules and monitored by resonance line absorption is a problem of general interest.

2. Experimental

A detailed description of the experimental arrangement has been given hitherto [7, 8]. We restrict our account here to the salient features of the apparatus and the procedure for the experimental measurements. $Pb(6^3P_0)$ was generated by the pulsed irradiation (E = 250 J, $\lambda > 165$ nm) of $PbEt_4$ in the presence of excess CO_2 ($p(CO_2)$:$p(PbEt_4)$ is approximately 10^5:1) in a coaxial lamp and vessel assembly to ensure optimum optical coupling between the photolysis source and the reaction cell. The lead atoms were then monitored by resonance line absorption at λ = 283.3 nm ($Pb(7s(^3P_1^0) \leftarrow 6p^2(^3P_0))$), $gA = 1.8 \times 10^8$ s^{-1} [12]) using a high intensity hollow cathode source (high spectral output Pb lamp, Westinghouse, U.S.A., operating voltage 1100 V, current 7 mA). After isolation of the atomic line (Seya–Namioka grating monochromator [13 - 15]), the photoelectric pulses (EMI photomultiplier tube 9783B) representing resonance line absorption were amplified without distortion [16] and were transferred to a transient recorder (Data Laboratories, DL 905) employed in the A/B mode [7, 8]. The signals were then digitized, stored and transferred onto paper tape (Datadynamics punch 1133) in ASCII code for direct input into the University of Cambridge IBM 370 computer. As described previously [7, 8], the data were subjected to the numerical smoothing procedure of Savitsky and Golay [17]. The resonance absorption signals were analysed using both the standard Beer–Lambert law

$$I_{tr} = I_0 \exp(-\epsilon c l) \qquad (I)$$

and the modified Beer–Lambert law [18]

$$I_{tr} = I_0 \exp \{-\epsilon(cl)^{\gamma}\} \quad \text{(II)}$$

using the previously determined value of $\gamma = 0.38 \pm 0.04$ [5] for the $\lambda = 283.3$ nm transition.

2.1. Materials

All materials ($PbEt_4$, CO_2, CO and Kr (for the photoflash lamp)) were prepared as described previously [17].

3. Experimental investigation

Previous studies [5 - 8] of the temporal behaviour of $Pb(6^3P_0)$ by resonance line absorption have been carried out in the regime of first order kinetics, namely where the decay could be described by the rate equation

$$\frac{-\mathrm{d} \ln\{Pb(6^3P_0)\}}{\mathrm{d}t} = k' = K + \Sigma k_R[R] \quad \text{(III)}$$

where R is any reactant gas and, in the absence of added gas, principally comprises the parent molecule $PbEt_4$ itself. k_R is the absolute second order rate constant for the reaction of $Pb(6^3P_0)$ with R. The term K (excluding the coefficient $k(PbEt_4)[PbEt_4]$), which includes first order contribution to the decay by diffusion, is small and can sensibly be neglected for most experimental conditions. Use of the first order kinetic regime enjoys, of course, the considerable advantage of avoiding a light absorption calibration involving the absolute concentration of $Pb(6^3P_0)$. The kinetic behaviour described by eqn. (III) will arise (a) when collisional relaxation of the optically metastable states $Pb(6^3P_1)$ (0.969 eV), $Pb(6^3P_2)$ (1.32 eV), $Pb(6^1D_2)$ (2.66 eV) and $Pb(6^1S_0)$ (3.65 eV) [19] that are generated in this type of experimental system has been completed and (b) when the concentration of $Pb(6^3P_0)$ is sufficiently low for the atomic recombination rate term $k_3[Pb]^2[M]$ (M = third body) to be negligibly small in comparison with the term $\Sigma k_R[R]$. The former condition can be satisfied by monitoring the lead atom over a time scale by which relaxation to the ground state is sensibly completed. This can readily be calculated from the appropriate collisional quenching rate constants [20 - 26]. The latter condition simply results from the use of suitably low pressures of the parent molecule $PbEt_4$ which are none the less commensurate with the production of measurable photochemical yields of atoms and from the use of relatively low pulse energies. It only requires an approximate curve-of-growth calculation [27], restricted to Voigt profiles for a single atomic line and a standard three-layer model [28, 29], to demonstrate the sensitivity of the resonance line absorption method for $Pb(6^3P_0)$. The present single-shot mode arrangement is capable of detecting lead atom concentrations of about 10^{10} atoms cm^{-3}. This sensitivity arises in part from the stability of the high spectral output hollow cathode spectroscopic source as opposed to a microwave-powered source which is character-

ized by a greater noise level. Hence the degrees of light absorption employed in previous measurements on $Pb(6^3P_0)$ [7, 8] indicate that the contribution to the decay of the lead atom from atomic recombination is negligible.

Experiments were performed in this investigation to monitor the decay of $Pb(6^3P_0)$ using the kinetic equation

$$\frac{-d[Pb]}{dt} = k_3[Pb]^2[M] + k'[Pb] \qquad (IV)$$

CO_2 was employed as the third body M on account of its relatively high efficiency in other atomic recombination processes [1]. A low pressure of CO ($p(CO) = 133$ N m^{-2}) was also employed in order to ensure efficient relaxation of $Pb(6^3P_1)$ and $Pb(6^3P_2)$ [20]. Under these conditions k' can be approximated to $k(PbEt_4)[PbEt_4]$. Clearly, the use of relatively high pressures of $PbEt_4$ to increase $[Pb(6^3P_0)]$ on photolysis and hence the magnitude of the term in $[Pb]^2$ will also result in an increase in the magnitude of the term $k'[Pb]$ (eqn. (IV)). The alternative is to employ relatively high pulse energies and lower concentrations of the parent molecule than used in the earlier experiments [7, 8] and to seek curvature in the first order kinetic decay traces.

Figure 1(a) gives an example of the digitized form of the computer output for the transmitted light intensity at $\lambda = 283.3$ nm, indicating the decay

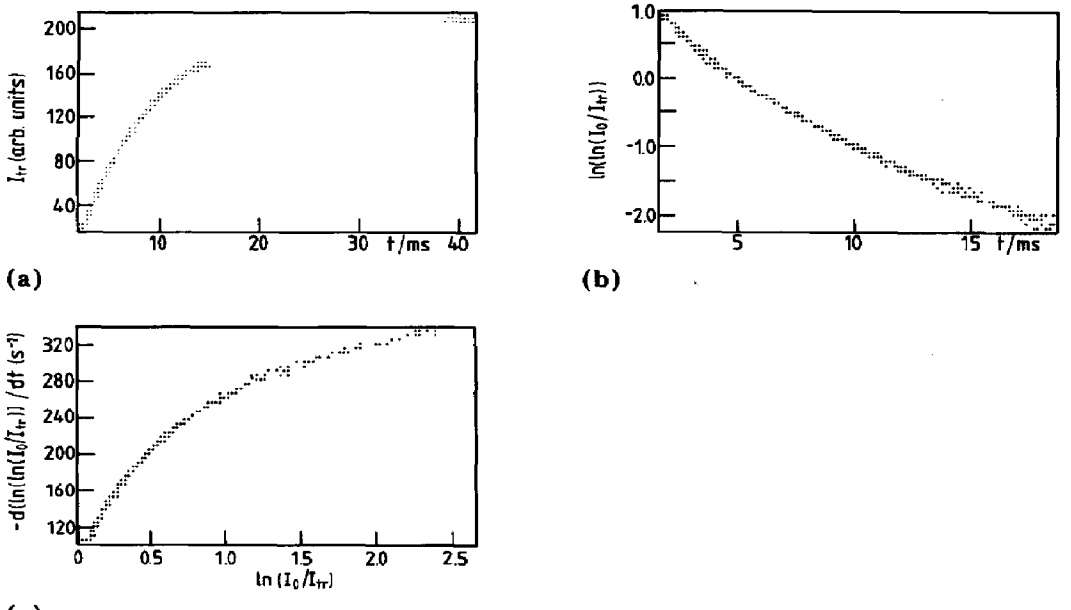

Fig. 1. Computerized output of experimental data in digital form resulting from resonance line absorption at $\lambda = 283.3$ nm ($Pb(7s(^3P_1^0) \leftarrow 6p^2(^3P_0))$) following the pulsed irradiation of $PbEt_4$: $[PbEt_4] = 1.8 \times 10^{13}$ molecules cm^{-3}; $[CO_2] = 1.2 \times 10^{18}$ molecules cm^{-3}; $[CO] = 9.6 \times 10^{16}$ molecules cm^{-3}; $E = 250$ J. (a) Numerically smoothed transmitted light intensity I_{TR} *vs.* time; (b) ln ln(I_0/I_{tr}) *vs.* time; (c) d ln ln(I_0/I_{tr})/dt *vs.* time.

of resonance absorption by $Pb(6^3P_0)$. Figure 1(b) shows a plot derived from the data of Fig. 1(a) assuming first order kinetic decay. There is clearly curvature at shorter times which obviously does not arise from any effects of physical relaxation into the $^3P_0$ state as the curvature so generated would occur in the opposite sense. For simplicity, we shall employ the Beer–Lambert law (eqn. (I)) to illustrate the order of magnitude involved in the kinetic analysis. (We emphasize that ϵ in eqn. (I) is the true extinction coefficient as opposed to that given in eqn. (II) where it is a floating variable of dimensions $(cl)^{-\gamma}$. It has the empirical meaning of being the slope of the curve of growth when given in logarithmic form, *i.e.* $\ln \ln(I_0/I_{tr})$ *versus* $\ln c$.) The combination of eqns. (I) and (IV) yields

$$\frac{\mathrm{d} \ln \ln(I_0/I_{tr})}{\mathrm{d}t} = -k' - \frac{k_3[\mathrm{M}]}{\epsilon l} \ln\left(\frac{I_0}{I_{tr}}\right) \qquad \text{(V)}$$

The left-hand side of eqn. (V) is the instantaneous value of the slope of the plot given in Fig. 1(b). As a result of the noise in a digitized plot, it was clearly necessary to reconvert the data of Fig. 1(b) into analogue form in order to obtain the slopes at different points. This was achieved by fitting a least squares cubic polynomial to every 20th point in Fig. 1(b) using the NAG library routine EO2ACF [30], the fit being accurate to 4% or less. Higher degree polynomials were found to be less suitable on account of their tendency to oscillate about the experimental curve. The instantaneous value of $\mathrm{d} \ln \ln(I_0/I_{tr})/\mathrm{d}t$ was then obtained from the computerized derivative of the cubic plot. The result, plotted against $\ln(I_0/I_{tr})$ (eqn. (V)), is shown in Fig. 1(c). The initial slope of this plot should yield a linear measure of $k_3[\mathrm{M}]$ which can be placed on an absolute basis by calculation of ϵ through the curve of growth. Sensible estimates of the atomic concentration both from the calculated curves of growth and from estimates of atomic yields on photolysis indicate that atomic recombination rates derived from the foregoing procedure are too rapid (see Section 4) by about four orders of magnitude. The curvature in Fig. 1(b) can sensibly be accounted for by rapid reaction of the lead atom with the fragments of the photolysis of $PbEt_4$. These results are fully in accord with previous failures [31] to observe Pb_2 in absorption in this type of system. A more complex analysis, in which the equivalents of Figs. 1(b) and 1(c) are constructed either from an empirically measured value of γ (eqn. (II)) or from a calculated value via the logarithmic form of the curve of growth, is not warranted in view of the disparity between the results for atomic recombination rates derived from the simple analysis presented and sensible values that may be expected. The effect of the high sensitivity of the resonance line absorption technique is that the kinetic component in $[Pb]^2$ is only significant compared with the first order decay term when the atomic line is effectively saturated. Hence the only convenient procedure at present is to calculate the atomic recombination rates from theory.

4. Calculation of the atomic recombination rate

The rate of recombination of two $Pb(6^3P_0)$ atoms in the presence of various third bodies M is calculated according to the phase space theory of Keck [10, 11]. It is assumed that the reaction surface is adiabatic and that the nuclear motion is described by classical mechanics. Any configuration of the three atoms is represented by a point in 18-dimensional phase space. The recombination rate is calculated by considering the crossing of a trial surface by points which represent separated $Pb(6^3P_0)$ atoms from those that are bound in Pb_2. The surface is only well defined in the region of phase space corresponding to configurations in which interactions are negligible and in such regions it must coincide with the surface used to calculate the equilibrium constant for Pb_2 dissociation. In regions where interactions between the three particles are important, the surface is not defined in this manner and can be chosen at will. Keck's theory incorporates a detailed and explicit consideration of the X–M ($Pb(6^3P_0)$–M) interaction, in contrast with the earlier phase space theory of Wigner [32], and also makes allowance for the centrifugal barrier in the effective potential operating between the two X ($Pb(6^3P_0)$) atoms. Advantage is taken of the arbitrary nature of the dividing surface which in Keck's theory forms the basis of a variational calculation, the surface being defined in terms of a single parameter which may be varied to give the minimum rate of crossing for the given overall form of the surface. Only the broad outline of the necessary mathematical development is given here. The full details may be seen in Keck's original paper [11].

The crossing rate R at which representative points in phase space cross a given surface S may be expressed as an integral

$$R = \int_S \rho(\boldsymbol{v}\cdot\boldsymbol{n})\mathrm{d}S \qquad \boldsymbol{v}\cdot\boldsymbol{n} > 0 \tag{1}$$

where ρ is the density of representative points, $\boldsymbol{v}$ is the generalized velocity of a representative point and $\boldsymbol{n}$ is the unit vector normal to the element $\mathrm{d}S$. The requirement that $\boldsymbol{v}\cdot\boldsymbol{n} > 0$ is, of course, equivalent to taking the rate of crossing of S in one direction only. We now suppose that the surface S can be defined in terms of the variables p_i, q_i of the phase space together with one or more adjustable parameters α_i by an equation of the form

$$\phi(p_i, q_i, \alpha_i) = 0 \tag{2}$$

On this basis, the unit vector $\boldsymbol{n}$ may be written

$$\boldsymbol{n} = \frac{\nabla\phi}{|\nabla\phi|} \tag{3}$$

and thus

$$R = \int_S \rho(\boldsymbol{v}\cdot\nabla\phi)\frac{\mathrm{d}S}{|\nabla\phi|} \tag{4}$$

In general, a value cannot be assigned to ρ, the density of points in the region of interest. The most convenient procedure is to use instead the maximum value ρ_m attained by ρ in regions of the phase space where interactions between the particles are unimportant, since as a result of Liouville's theorem $\rho < \rho_m$. The effect of employing ρ_m instead of ρ will result in an upper bound to the value of R, namely

$$R_m = \int_S \rho_m (\boldsymbol{v} \cdot \nabla \phi) \frac{dS}{|\nabla \phi|} \tag{5}$$

The scalar product may be expanded as

$$R_m = \sum_i \int_{\substack{S \\ v \cdot n > 0}} \rho_m \left(\dot{p}_i \frac{\partial \phi}{\partial p_i} + \dot{q}_i \frac{\partial \phi}{\partial q_i} \right) \frac{dS}{|\nabla \phi|} \tag{6}$$

and, from Hamilton's equations,

$$\frac{\partial H}{\partial q_i} = -\dot{p}_i \qquad \frac{\partial H}{\partial p_i} = \dot{q}_i$$

where H is the total energy; then

$$R_m = \sum_i \int_S \rho_m \left(- \frac{\partial H}{\partial q_i} \frac{\partial \phi}{\partial p_i} + \frac{\partial H}{\partial p_i} \frac{\partial \phi}{\partial q_i} \right) \frac{dS}{|\nabla \phi|} \tag{7}$$

It is evident that the term in parentheses in eqn. (7) is simply

$$\begin{vmatrix} \dfrac{\partial H}{\partial p_i} & \dfrac{\partial H}{\partial q_i} \\ \dfrac{\partial \phi}{\partial p_i} & \dfrac{\partial \phi}{\partial q_i} \end{vmatrix}$$

which is, by definition, the Jacobian for the transformation from (H,ϕ) coordinates to (p_i, q_i) coordinates: $\partial(H,\phi)/\partial(p_i, q_i) = \mathcal{J}_i$. Thus

$$R_m = \sum_i \mathcal{J}_i' \int_S \rho_m \frac{dH\, d\phi\, dS}{dp_i\, dq_i\, |\nabla \phi|} \tag{8}$$

where

$$\mathcal{J}_i' = \frac{\partial(H,\phi)/\partial(p_i,q_i)}{|\partial(H,\phi)/\partial(p_i,q_i)|} \qquad \text{if} \quad \frac{\partial(H,\phi)}{\partial(p_i,q_i)} \neq 0$$

otherwise $\mathcal{J}_i' = 0$.

Equation (8) may be simplified since dS is an element of the surface S and $d\phi/|\nabla\phi|$ is a vector normal to it. Thus, $d\phi dS/|\nabla\phi|$ represents an element of volume which in terms of p_i and q_i is given by

$$\frac{\mathrm{d}S\mathrm{d}\phi}{|\nabla\phi|} = \prod_{k\neq i} \mathrm{d}p_k\,\mathrm{d}q_k$$

where the exclusion from the product of $\mathrm{d}p_i\mathrm{d}q_i$ is of course due to the fact that $\mathrm{d}p_i\mathrm{d}q_i$ appears in the denominator of eqn. (8). Thus we have

$$R_{\mathrm{m}} = \sum_i \mathcal{J}_i' \int_S \rho_{\mathrm{m}}\,\mathrm{d}H \prod_{k\neq i} \mathrm{d}p_k\,\mathrm{d}q_k \tag{9}$$

Furthermore, for a gas in thermodynamic equilibrium

$$\rho_{\mathrm{m}} = \rho_0 \exp\left(-\frac{H}{kT}\right) \tag{10}$$

where ρ_0 is a constant.

The remaining development leading to the final expression for the variational rate constant has as its starting point eqns. (9) and (10) in conjunction with a suitable choice of coordinate system and trial surface.

Apart from the use of ρ_{m} for ρ, there are two other principal reasons why R_{m} constitutes an upper bound to the rate. Firstly, the effect of trajectories which cross S more than once has been overlooked and is likely to be particularly important at high temperatures. Secondly, it is possible that some parts of the surface S will not be accessible to trajectories which originate from regions of the phase space far from the zone where interactions are important.

Before proceeding to the equations which are the end result of the mathematical development based on eqns. (9) and (10) it is necessary to consider the nature of the trial surface used by Keck [11] and to discuss the manner in which the three-body potential is treated. Clearly, one cannot represent diagramatically a surface in 18-dimensional space but one can represent it in the three-dimensional space whose axes are H_{12}, r_{12}, and r_3 where r_{12} is the distance between X_1 and X_2 (the two Pb atoms), r_3 is the distance of M from the centre of mass of X_1–X_2 and H_{12} is the internal energy of X_1–X_2. (The original 18 dimensions are, of course, implicit in such a representation.) The internal energy of X_1–X_2 can be written

$$H_{12} = \frac{p_{12}^2}{2\mu_{12}} + \frac{l_{12}^2}{2\mu_{12}r_{12}^2} + V_{12}(r_{12})$$

where p_{12} is the linear momentum of X_1–X_2, μ_{12} is the reduced mass, l_{12} is the angular momentum and V_{12} is the potential energy. The latter two terms in H_{12} define the effective potential V_{eff} since the term in l_{12}^2 represents the presence of a centrifugal barrier. The barrier occurs at $r_{12} = z$ where

$$\left(\frac{\partial V_{\mathrm{eff}}}{\partial r_{12}}\right)_{r_{12}=z} = 0$$

which at $r_{12} = z$ yields

$$\frac{\partial V_{12}(r_{12})}{\partial r_{12}}\left(\frac{-l_{12}^2}{\mu r_{12}^3}\right) = 0$$

and, in turn,

$$\left(\frac{\partial V_{12}(r_{12})}{\partial r_{12}}\right)_z = \frac{l_{12}^2}{\mu_{12} z^3}$$

Hence

$$V_{\text{eff}}\,(\max) = B = V_{12}(z) + \frac{1}{2} z \left(\frac{\partial V_{12}(r_{12})}{\partial r_{12}}\right)_z$$

i.e. the position and energy of the rotational barrier are defined by z and B. Given these parameters, the trial surface in H_{12}–r_{12}–r_3 space can be defined in terms of the variational parameter a and there are two faces to the surface:

face (a) $\quad r_3 = a, \quad H_{12} \leqslant B, \quad r_{12} \leqslant z$

face (b) $\quad r_3 \geqslant a, \quad H_{12} = B, \quad r_{12} \leqslant z$

This is represented diagrammatically in Fig. 2.

The decomposition of the trial surface into two distinct faces in this way reduces the final result into the sum of two terms corresponding to crossings of the faces. The rate at which representative points cross face (a) is equivalent to the rate of binary collisions between $X_1 X_2$ and M, the variational parameter a being regarded as a collision diameter. What is required is the rate of such collisions in which there is sufficient energy to dissociate $X_1 X_2$. This component of the solution has been termed the "available energy" rate by Keck [11]. Crossings of face (b) are analogous to the approach of Wigner [32] with the added effect of the centrifugal barrier in the effective

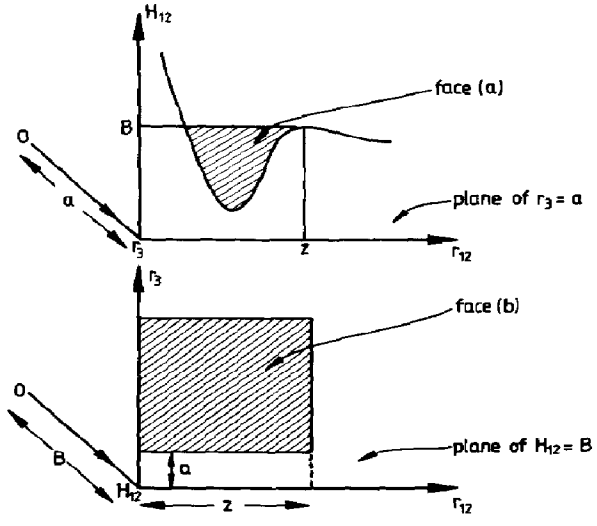

Fig. 2. Schematic two-dimensional representation of the trial surface for the variational phase space calculation of atomic recombination rates.

potential, the corresponding rate being termed the "barrier rate", again following Keck [11]. It will be seen that in the present calculations it is the latter rate which determines the overall variational rate constant.

As stated previously, the full details of the procedures leading to the final expressions used in the calculations will not be given here but simply the equations used together with some brief explanatory comments. The equations used are as follows.

(a) The available energy component k_A is given by

$$k_A(a) = \frac{4\pi a^2 r_0^2 g_{12}}{g_1 g_2 \beta_{12}} (\cos\alpha_- - \cos\alpha_+) \left(\frac{2D_{12}}{\mu_3}\right)^{1/2} \left\{\frac{1}{2}\left(\frac{D_{12}}{kT}\right) + \frac{1}{6}\left(\frac{D_{12}}{kT}\right)^2\right\} \quad (11)$$

in which a is the variational parameter, g_{12}, g_1 and g_2 are the electronic degeneracies of X_1X_2, X_1 and X_2, r_0 is the equilibrium distance in the diatomic molecule, β_{12} and D_{12} are the parameters in the Morse potential for X_1X_2, μ_3 is the reduced mass of $M + X_1X_2$ and α_- and α_+ are two angles which allow for the requirement that M is excluded from regions where $V_{total} > 0$.

(b) The barrier component k_B is given by

$$k_B(a) = \frac{2\pi g_{12}}{g_1 g_2} (2\pi\mu_{12}kT)^{1/2} (z_2 - z_1) z_2^2 \left\{1 - \exp\left(\frac{-B_m}{kT}\right)\right\} \times$$

$$\times \frac{2}{m_{Pb}} \left[a_-^2 (F_1 + F_2) \exp\left(\frac{\epsilon}{kT}\right) + a_+^2 (F_3 + F_4)\left\{\exp\left(\frac{\epsilon}{kT}\right) - 1\right\}\right] \quad (12)$$

where ϵ is the Lennard-Jones well depth for the X–M interaction, a_- and a_+ are the two values of r_{13} for which $(1/kT)(du/dr) \exp(-u/kT)$ has a maximum ($u = V_{Pb-M}$), z_2 is the value of z for which $(db/dr) \exp(-b)$ has a maxumum ($b = B/kT$ where B has been defined previously) and z_1 is the value of r_{12} at which the repulsive portion of V_{eff} cuts $V = B$. F_1 - F_4 are integrals with respect to z which effectively account for the solid angles over which M can induce vibrational and rotational transitions in X_1–X_2. The limits of these integrals are z_1 (lower) and z_2 (upper). Since the integrands are somewhat complex, they will not be reproduced here. Finally, there will be a maximum value of l_{12} above which the rotational barrier ceases to exist; the corresponding value of B is then B_m in eqn. (12).

As it is extremely difficult to construct a realistic three-body potential, especially in this system, the procedure adopted in this theory is to assume separability, so that

$$V_{total} \approx V_{12}(r_{12}) + V_{13}(r_{13}) + V_{23}(r_{23})$$

and to use suitable expressions for the two-body potentials. The Pb–Pb interaction $V_{12}(r_{12})$ is represented by the Morse function

$$V(r) = D_{12}[1 - \exp\{-\beta_{12}(r - r_0)\}]^2$$

with $D_{12} = 9.61 \times 10^{-13}$ erg, $\beta_{12} = 4.56 \times 10^8$ cm^{-1} and $r_0 = 3.08$ Å [33]. For the remaining interactions (Pb–M) two procedures are used, one for the

inert gases and the other for the diatomic and polyatomic molecules. Firstly, when M is an inert gas, van der Waals' interaction is represented by the Lennard-Jones 12–6 potential and the repulsive short range interaction is represented by the Mason–Vanderslice potential [34]. Provided that $V/D \ll 1$ [34], as is the case here, this potential can be written

$$V(r) = D \exp \{-\beta r - 2\alpha \exp (-\beta r/\alpha)\}$$

Suitable values of D, β and α for the inert gases have been given by Mason and Vanderslice [34]. In the cases for which M is a diatomic or polyatomic molecule, the Lennard-Jones 12–6 potential is used at all distances to represent the Pb–M interaction, employing the standard geometric mean rule. All the parameters used [33 - 35] are listed in Table 1; those for Pb were obtained by extrapolation of the values for the inert gases on the basis of atomic number.

We stress that the theory is only strictly valid if M is a monatomic chaperone. However, provided that the recombination of Pb atoms proceeds largely via a radical complex mechanism (*i.e.* energy transfer is not important), the rate will depend not so much on the internal complexity of M as on the volume of configuration space available to the Pb–M pair as evidenced by the strength of their interaction.

The calculations of k_A and k_B from eqns. (11) and (12) were performed on the University of Cambridge IBM 370 computer using a program which was first checked against calculations on the reaction O + O + Ar [11] and was found to reproduce the previously reported values satisfactorily. The integrals F_1 - F_4 in the expression for the barrier rate were evaluated using

TABLE 1

Parameters used in calculations of interatomic potentials

M	Lennard-Jones		Mason–Vanderslice		
	ϵ (erg)	σ(Å)	D (erg)	β (cm^{-1})	α
He	1.38×10^{-15}	2.60	5.67×10^{-10}	4.38×10^{8}	1.50
Ne	4.55×10^{-15}	2.79	2.18×10^{-9}	4.24×10^{8}	1.54
Ar	1.65×10^{-14}	3.42	2.11×10^{-9}	3.10×10^{8}	2.18
Kr	2.38×10^{-14}	3.60	3.28×10^{-9}	2.74×10^{8}	2.39
Xe	3.07×10^{-14}	4.04	3.74×10^{-9}	2.38×10^{8}	2.24
N_2	1.26×10^{-14}	3.68			
O_2	1.56×10^{-14}	3.43			
CO_2	2.62×10^{-14}	3.99			
SF_6	2.77×10^{-14}	5.51			
CF_4	2.10×10^{-14}	4.70			
CH_4	1.89×10^{-14}	3.82			
C_2H_6	3.17×10^{-14}	4.42			
Pb	3.86×10^{-14}	4.65	4.83×10^{-9}	1.8×10^{8}	2.90

Morse parameters used for Pb_2: $D = 9.61 \times 10^{-13}$ erg, $r_0 = 3.08$ Å and $\beta = 4.56 \times 10^{8}$ cm^{-1}.

Patterson's modification of the method of Gaussian quadrature (NAG library routine DO1ACF) [36]; otherwise, the computational procedure is lengthy but straightforward. Typical results from the program are shown in Figs. 3 and 4 in which k_A and k_B are plotted against the function $f(a) = \{a/(a_- + z_m/2)\}^2$ where a_- has been defined previously and z_m is the value of z corresponding to the maximum rotational barrier height B_m. This device merely serves to give some degree of normalization. Values of k_A and k_B were calculated for

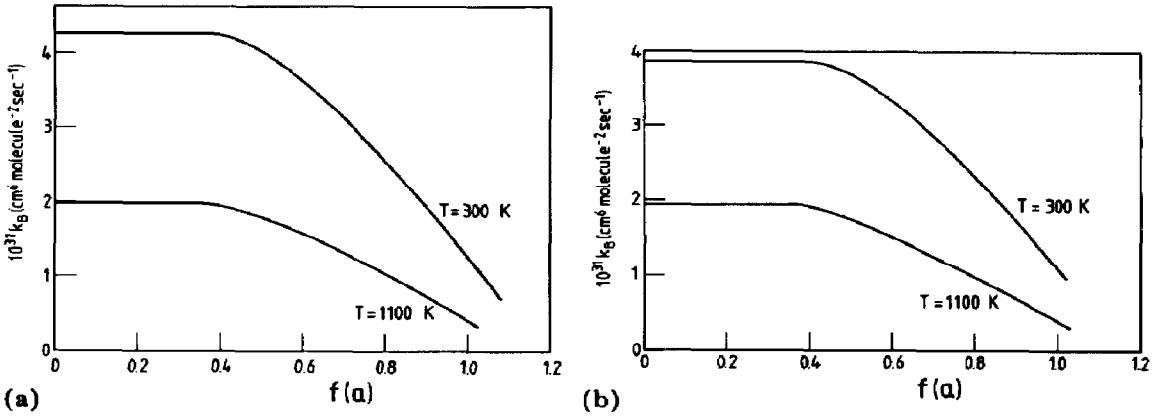

Fig. 3. Plots of the barrier component k_B of the variational rate constant *vs.* the function $f(a)$ of the variational parameter a (see text) for the recombination of Pb (6^3P_0) in the presence of (a) xenon and (b) CO_2 at T = 300 and 1100 K.

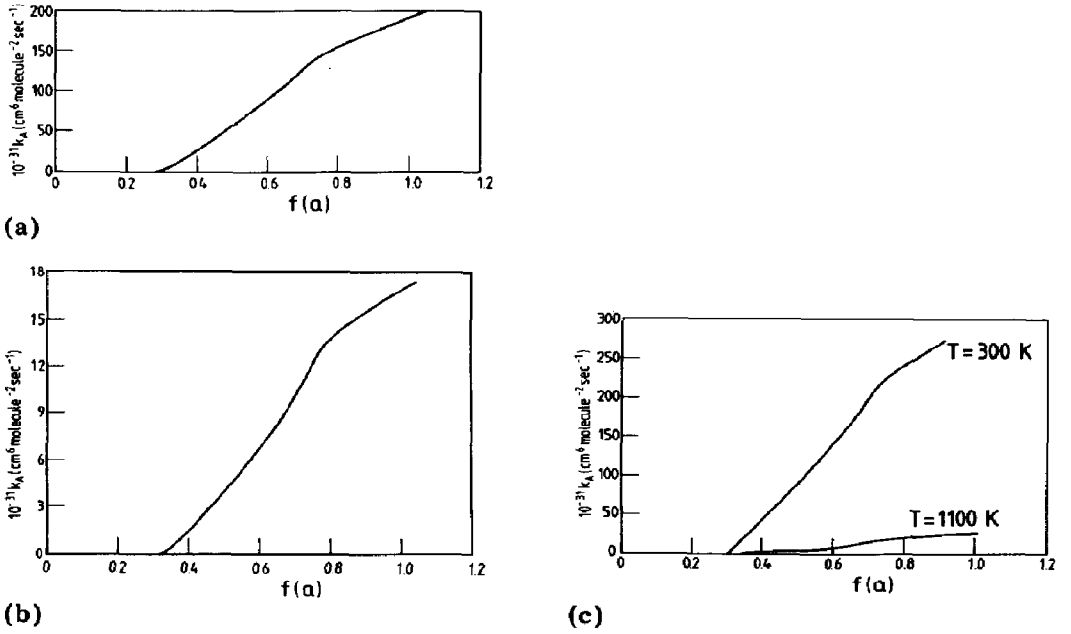

Fig. 4. Plots of the available energy component k_A of the variational rate constant *vs.* the function $f(a)$ for the recombination of Pb(6^3P_0) in the presence of (a) xenon at T = 300 K, (b) xenon at T = 1100 K and (c) CO_2 at T = 300 and 1100 K.

various values of $f(a)$ between 0 and 1. Several features of the solutions are worthy of note. Firstly, the overall least upper bound k is given in each case by the value of k_B for $a = 0$ because k_A vanishes at $a = 0$. Above a certain value of a, however, k_A rises very steeply indeed. This threshold effect in k_A is due to the operation of the term $(\cos \alpha_- - \cos \alpha_+)$ in eqn. (11); for small values of a the sphere on which M lies, and which is centred on the midpoint of the internuclear axis X_1–X_2, is wholly contained in the region for which $V_{total} > 0$, but as a increases the sphere expands to admit the region of $V < 0$. Above a certain value of a the sphere is sufficiently large for this restriction to be no longer operative, *i.e.* $V_{total} < 0$ everywhere on the sphere and k_A is simply proportional to a^2 as evidenced by the linear portion of k_A *versus* $f(a)$ near $f(a) = 1$. Indeed, this portion would, if projected back to $a = 0$, go through the origin. By contrast, the barrier component has its maximum value at $a = 0$ since the solid angle terms implicit in the integrals F_1 - F_4 are largest here but fall off as a increases. In all cases therefore the variational rate constant k is equal to k_B at $a = 0$ and the values calculated for various M are given in Table 2 for $T = 300$, 850 and 1100 K.

It can be seen that several general experimental observations [1] are reproduced satisfactorily by Keck's theory [11]: firstly, the reaction rate decreases with increasing temperature; secondly, the trend in rate constant as M proceeds, for example, from He to Xe cannot be explained simply by the effect of the size of M (hence the failure of Wigner's calculation on this point [32]); thirdly, the temperature dependence is strongest for those types of M that are most efficient at low temperature.

Finally, we return to the nucleation of lead. Homer and Prothero [4] have given a detailed parameterized mathematical model for the nucleation process in order to account for their observations following the shock-tube-initiated thermal decomposition of tetramethyl lead. Further, a simple

TABLE 2

Third order rate constants k_3 (10^{-32} cm^6 molecule^{-2} s^{-1}) for Pb + Pb + M calculated according to the phase space variational method of Keck [11]

M	T = 300 K	T = 850 K	T = 1100 K
He	9.9	8.7	8.5
Ne	14.4	10.8	10.4
Ar	27.3	16.2	15.0
Kr	34.2	18.7	17.3
Xe	42.6	22.1	19.9
N_2	25.6	16.2	15.1
O_2	26.7	16.3	15.0
CO_2	38.9	20.9	19.0
CF_4	39.6	22.4	20.6
SF_6	52.8	28.0	25.4
CH_4	31.7	18.4	16.9
C_2H_6	47.0	24.0	21.7

mechanistic description from the chemical viewpoint [4] indicated that an upper limit for the nucleation rate could be derived from the atomic recombination rate of lead atoms. In the absence of data for the Pb atoms, the recombination rate was estimated from established data for I + I + Ar which yielded a nucleation rate a factor of 3 higher than that observed [4]. Homer and Prothero concluded that the reaction from Pb + Pb + M was probably not the rate-determining step. The present work shows that the upper limit for the nucleation rate calculated on the basis of atomic recombination is higher by at least an order of magnitude. Keck's theory [11] certainly accounts well for I atom recombination rates in noble gases [37]. The rates for Pb + Pb + M calculated for noble gasses are higher by about a factor of 35. Hence, Homer and Prothero's suggestion [4] can be regarded as probably being correct and an alternative chemical step must be the rate-determining process.

Acknowledgment

We thank the Science Research Council of Great Britain and the Associated Octel Company for the award of a C.A.S.E. Studentship to one of us (P.J.C.), during the tenure of which this work was carried out.

References

1 W. Jost (ed.), Physical Chemistry, an Advanced Treatise, Vol. VIA, Kinetics of Gas Reactions, Academic Press, New York, 1974.
2 W. Jost (ed.), Physical Chemistry, an Advanced Treatise, Vol. VIB, Kinetics of Gas Reactions, Academic Press, New York, 1975.
3 E. E. Nikitin, Theory of Elementary Atomic and Molecular Processes in Gases, Clarendon Press, Oxford, 1974.
4 J. B. Homer and A. Prothero, J. Chem. Soc. Faraday Trans. 1, 69 (1973) 673.
5 D. Husain and J. G. F. Littler, J. Photochem., 2 (1973/74) 247.
6 D. Husain and J. G. F. Littler, Combust. Flame, 22 (1974) 295.
7 P. J. Cross and D. Husain, J. Photochem., 7 (1977) 157.
8 P. J. Cross and D. Husain, J. Photochem., 8 (1978) 183.
9 D. Husain, Ber. Bunsenges. Phys. Chem., 81 (1977) 168.
10 J. C. Keck, J. Chem. Phys., 29 (1958) 410.
11 J. C. Keck, J. Chem. Phys., 32 (1960) 1035.
12 C. H. Corliss and W. R. Bozman, Experimental transition probabilities for spectral lines of seventy elements, Nat. Bur. Stand. (U.S.), Monogr., 53, 1962.
13 M. Seya, Sci. Light (Tokyo), 2 (1952) 8.
14 T. Namioka, Sci. Light (Tokyo), 3 (1954) 15.
15 M. J. Bevan and D. Husain, J. Photochem., 3 (1974/75) 1.
16 W. H. Wing and T. M. Sanders Jr., Rev. Sci. Instrum., 38 (1962) 1341.
17 A. Savitsky and J. E. Golay, Anal. Chem., 36 (1964) 1627.
18 R. J. Donovan, D. Husain and L. J. Kirsch, Trans. Faraday Soc., 66 (1970) 2551.
19 C. E. Moore (ed.), Atomic Energy Levels, Vols. I - III, Nat. Bur. Stand., Circ., 467, 1958.
20 D. Husain and J. G. F. Littler, Int. J. Chem. Kinet., 6 (1974) 61.

21 J. J. Ewing, Chem. Phys. Lett., 29 (1974) 50.
22 J. J. Ewing, D. W. Trainor and S. Yatsiv, J. Chem. Phys., 61 (1974) 4433.
23 D. Husain and J. G. F. Littler, Chem. Phys. Lett., 16 (1972) 145.
24 D. Husain and J. G. F. Littler, J. Chem. Soc. Faraday Trans 2, 68 (1972) 2110.
25 D. Husain and J. G. F. Littler, J. Photochem., 1 (1973) 327.
26 D. Husain and J. G. F. Littler, J. Chem. Soc. Faraday Trans. 2, 69 (1973) 842.
27 A. C. G. Mitchell and M. W. Zemansky, Resonance Radiation and Excited Atoms, Cambridge University Press, London, 1934.
28 W. Braun and T. Carrington, J. Quant. Spectrosc. Radiat. Transfer, 9 (1968) 1133.
29 L. F. Phillips, Chem. Phys. Lett., 37 (1976) 421.
30 NAG Subroutine Library, Mk. 5, 1976.
31 D. Husain and J. G. F. Littler, unpublished results.
32 E. P. Wigner, J. Chem. Phys., 5 (1937) 720.
33 G. Herzberg, Spectra of Diatomic Molecules, Van Nostrand, New York, 1960.
34 E. A. Mason and J. T. Vanderslice, J. Chem. Phys., 28 (1958) 432.
35 J. O. Hirschfelder, C. F. Curtiss and R. B. Bird, Molecular Theory of Gases and Liquids, Wiley, New York, 1954.
36 T. N. L. Patterson, Math. Comput., 22 (1968) 847.
37 G. Porter, Discuss. Faraday Soc., 33 (1962) 198.